Monthly Notices
of the
ROYAL ASTRONOMICAL SOCIETY

Mon. Not. R. Astron. Soc. **414,** 1715–1720 (2011) doi:10.1111/j.1365-2966.2011.18505.x

Supernova shock breakout through a wind

Shmuel Balberg[1,2]★ and Abraham Loeb[1]

[1]*Harvard-Smithsonian Center for Astrophysics, 60 Garden Street, Cambridge, MA 02138, USA*
[2]*Racah Institute of Physics, The Hebrew University, Jerusalem 91904, Israel*

Accepted 2011 February 8. Received 2011 February 4; in original form 2011 January 13

ABSTRACT

The breakout of a supernova shock wave through the progenitor star's outer envelope is expected to appear as an X-ray flash. However, if the supernova explodes inside an optically thick wind, the breakout flash is delayed. We present a simple model for estimating the conditions at shock breakout in a wind based on the general observable quantities in the X-ray flash light curve; the total energy $E_{\rm X}$, and the diffusion time after the peak, $t_{\rm diff}$. We base the derivation on the self-similar solution for the forward–reverse shock structure expected for an ejecta plowing through a pre-existing wind at large distances from the progenitor's surface. We find simple quantitative relations for the shock radius and velocity at breakout. By relating the ejecta density profile to the pre-explosion structure of the progenitor, the model can also be extended to constrain the combination of explosion energy and ejecta mass. For the observed case of XRO08109/SN2008D, our model provides reasonable constraints on the breakout radius, explosion energy and ejecta mass, and predicts a high shock velocity which naturally accounts for the observed non-thermal spectrum.

Key words: shock waves – supernovae: general – supernovae: individual: SN 2008D – stars: winds, outflows.

1 INTRODUCTION

As a supernova shock wave propagates through the progenitor star, it eventually emerges through the outer envelope region which has a low optical depth. At this point the shock 'breaks out' of the star, initiating the first electromagnetic signal of the explosion. The breakout results in a flash of radiation, as the internal energy deposited by the shock diffuses out of the shocked region on a time-scale comparable to the dynamical time of the shock. Following breakout the ejected envelope expands so that the photosphere recedes into the ejecta. Any remaining internal energy, which has not been converted during adiabatic expansion, is then gradually radiated to power the supernova light curve.

It has long been suspected that the shock breakout from a star would appear as an X-ray flash (Colgate 1974; Klein & Chevalier 1978), followed by a ultraviolet (UV)/optical transient corresponding to emission from the outer layers of the ejecta (Falk 1978). The interest in prompt signals from supernovae increased recently due to the new capabilities of modern searches for transients, such as Pan-STARRS[1] and PTF[2] as well as the planned LSST[3] and WFIRST.[4] In fact, several supernovae light curves were observed early after the explosion both in the UV and the optical bands (Gezari et al. 2008, 2010; Soderberg et al. 2008). In two cases, GRB060218/SN2006aj (Campana et al. 2006) and XRO08109/SN2008D (Soderberg et al. 2008), X-ray detectors on board the *Swift* satellite have captured a luminous X-ray outburst, which were later followed by observations of supernovae in the longer wavelengths. Both events may very well have been the signature of shock breakout.

These new observations motivated detailed theoretical modelling of the early emission in supernovae. The models focused on the early UV/optical light curve that follows breakout, on time-scales of the order of a day (Chevalier & Fransson 2008; Nakar & Sari 2010; Rabinak & Waxman 2011), for which the dynamics are somewhat simpler (see also Chevalier 1992). Modelling the X-ray flash associated with breakout is more complicated, since it must include the properties and structure of the radiation-mediated shock (RMS) as it propagates through the sharply decreasing density of the outer envelope, where the shock width becomes non-negligible relative to the distance to the edge of the star. Katz, Budnik & Waxman (2010) have shown that if the shock velocity normalized by c, $\beta_{\rm S} \geq 0.07$, free–free emission will be unable to produce a large enough number density of photons to establish a blackbody spectrum. As a result, the average photon energy in the shocked region will be significantly larger than the equilibrium blackbody photon temperature with the same energy density. Hence, any analysis of the breakout light curve based on the assumption of local thermodynamic equilibrium and a blackbody spectrum will not reproduce the photon flux and spectrum emitted from the shock region during breakout.

★E-mail: shmblbrg@phys.huji.ac.il
[1] http://pan-starrs.ifa.hawaii.edu
[2] http://www.astro.caltech.edu/ptf/
[3] http://www.lsst.org/lsst
[4] http://wfirst.gsfc.nasa.gov/

The shock-breakout light curve could be significantly influenced by any circumstellar material (CSM) surrounding the exploding star. In fact, the aforementioned two candidates for an X-ray flash of a shock-breakout origin are associated with a Type Ibc supernova, in which the progenitor is believed to be a Wolf–Rayet star that has undergone significant mass-loss prior to the explosion. General, order of magnitude estimates for the energy enclosed in shock breakout do indeed favour a wind environment over a bare star in both cases (Waxman, Mészáros & Campana 2007; Chevalier & Fransson 2008; Katz et al. 2010). If the supernova takes place in an optically thick wind, the breakout is delayed from the observer's point of view, and the X-ray flash emerges only when the shock width in the wind becomes comparable to its distance from the CSM photosphere. Even a dynamically unimportant wind (which does not influence the emission of the early UV/optical light curve), will completely change the properties of the X-ray flash relative to a bare star by virtue of its optical depth.

Motivated by these considerations, we present here a simple analysis that relates the observable properties of the X-ray flash to the physical parameters of shock breakout in an optically thick wind. While a self-consistent treatment of the shock structure, light travel time and frequency dependence is required to reproduce the light curve of the flash, the integral quantities should be weakly dependent of these details. We apply the known self-similar solution of a supernova ejecta moving into a pre-existing wind material with a density profile of $\rho \propto r^{-2}$ (Chevalier 1982), and demonstrate how it can be used to relate the key observable features of the X-ray flash, the total energy $E_{\rm X}$ and the diffusion time-scale $t_{\rm diff}$ to the parameters of the shock breakout. Most notably, we can obtain a quantitative estimate of the breakout radius and the associated shock velocity. Our model expands upon the order of magnitude estimate presented by Ofek et al. (2010) regarding PTF09uj, which possibly exhibited a long (∼1 week) UV flash due to breakout in a very dense wind. While our model assumes a non-relativistic shock, it can be generalized to relativistic shocks and more complex wind structures, and also compared to the specific model suggested by Li (2007) for SN2006aj (note, however, that this source may have been significantly asymmetric, Waxman et al. 2007).

The outline of the paper is as follows. In Section 2 we review the self-similar solution for an ejecta expanding into a wind, and discuss the applicability of this physical setting to the problem of shock breakout. In Section 3 we present how the self-similar solution can be used to relate the observed properties of the X-ray flash to the conditions at breakout. In Section 4 we demonstrate that based on the initial profile of the ejecta (Matzner & McKee 1999), the observable quantities can be used to place constraints on the parameters of the underlying explosion. In Section 5 we consider the particular example of SN2008D, which is a borderline case in terms of the applicability of our model. Finally, Section 6 summarizes our main conclusions.

2 THE FORWARD–REVERSE SHOCK STRUCTURE

We consider a spherically symmetric supernova explosion in a nearly stationary CSM, produced by a wind from the progenitor star. The wind is assumed to be much slower than the ejecta. For a steady wind with a mass-loss rate $\dot{M}$ and a velocity $v_{\rm w}$, the density profile outside of the star is,

$$\rho(r) = \frac{\dot{M}}{4\pi r^2 v_{\rm w}} \equiv K r^{-2}. \quad (1)$$

Following the explosion, the outgoing ejecta plows through the wind material and slows down, driving a forward shock through the wind and a reverse shock that propagates back into the ejecta. Once the shock had propagated far enough from the star's surface so that the crossing time and the size of the star can be neglected, one may assume an asymptotic time-dependent density profile for the outer part of the supernova ejecta of the form,

$$\rho_{\rm e} = g^m r^{-m} t^{m-3}, \quad (2)$$

where g and m are constants which depend on the initial conditions of the progenitor and the explosion. If both the ejecta and the wind material are initially cold, a self-similar solution can be found to describe for the structures of both the forward shock (Parker 1963) and the reverse shock (Chevalier 1982). At any time, the flow consists of a forward-shock region of the swept up wind material, and a reverse shock in a leading region of the ejecta. At the boundary between the two regions, velocity and pressure are continuous but density is not. Denoting the position of the forward shock by $R_{\rm F}$, the reverse shock by $R_{\rm R}$ and the contact radius by $R_{\rm C}$, the ratios $R_{\rm R}/R_{\rm F}$ and $R_{\rm C}/R_{\rm F}$ are time independent. The solutions are found by integrating dimensionless functions of similarity variable, $\eta = r^{1/\lambda} t^{-1}$, where $\lambda = (m-2)/(m-3)$. The forward- and reverse-shock fronts serve as boundary conditions. Integration is carried out up to $R_{\rm C}$ from both ends, and the solutions are joined by matching the velocities and pressures on both sides of the contact surface.

The self-similar solution describes the normalized profiles of the density, velocity and pressure profiles as a function of η, and depends on the values of m and the adiabatic index of the shocked materials, γ. An example of such a profile for $m = 10$ and $\gamma = 4/3$ is presented in Fig. 1, where all quantities are normalized to their values just behind the forward shock. The gradual divergence of density at the discontinuity (in both of the forward and reverse shock regions) is generic to the assumed r^{-2} wind profile (Chevalier 1982), for which the solutions lead to a vanishing speed of sound on both sides of the contact radius. In reality, the divergence will be avoided since the density discontinuity is Rayleigh–Taylor unstable and hence the contact region will obtain a finite width.

Our choice of $\gamma = 4/3$ is, of course, motivated by our assumption that the shocks involved are radiation dominated; the internal energy

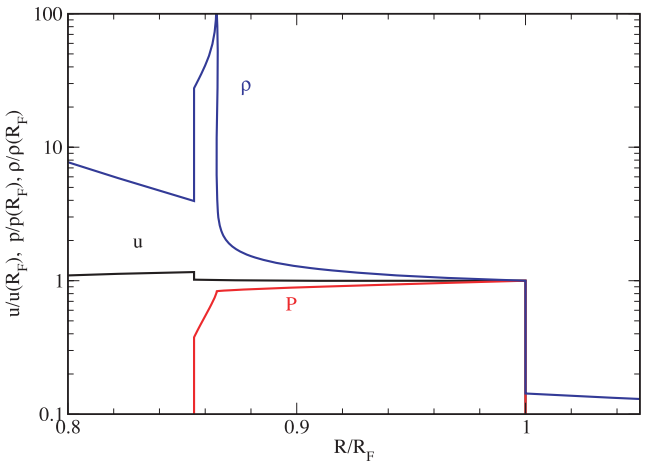

Figure 1. The velocity (black), pressure (red) and density (blue) profiles of the self-similar solution for supernova ejecta propagating through a wind with $m = 10$ and $\gamma = 4/3$ (see text). The radial coordinate is normalized to the radius of the forward shock, $R_{\rm F}$, and the physical quantities are normalized to their postshock values at the forward shock front.

density in the shocked region is therefore $\varepsilon = 3P$, where P is the pressure (see Chevalier 1983 for comparison, with $\gamma = 4/3$ motivated by cosmic-ray dominated shocks). By integrating over the pressure in the solution we can find the total energy in radiation. The pressure behind the forward shock, $P_{\rm F}$, is determined by the strong-shock condition,

$$P_{\rm F} = \frac{6}{7} K R_{\rm F}^{-2} \dot{R}_{\rm F}^2, \tag{3}$$

where $\dot{R}_{\rm F}$ is the velocity of the forward shock. Denoting the relative width of the shocked region by $x = (R_{\rm F} - R_{\rm R})/R_{\rm F}$ we may express the total internal energy in the shocked region as

$$E_{\rm rad}(x, R_{\rm F}) = \int_{R_{\rm R}}^{R_{\rm F}} 4\pi r^2 \varepsilon(r)\,{\rm d}r = \chi_{\rm E} \frac{72\pi}{7} K R_{\rm F} x \dot{R}_{\rm F}^2. \tag{4}$$

The dimensionless quantity $\chi_{\rm E}$ is defined by

$$\chi_{\rm E} = \frac{\int_{R_{\rm R}}^{R_{\rm F}} 4\pi r^2 P(r)\,{\rm d}r}{4\pi R_{\rm F}^3 x P_{\rm F}}, \tag{5}$$

and is determined by the details of the postshock profile. For the particular case of $m = 10$ and $\gamma = 4/3$ depicted in Fig. 1, $x = 0.146$, $\chi_{\rm E} = 0.9$.

The total width x is dominated by the forward shock region, which has a width of $x_{\rm F} = (R_{\rm F} - R_{\rm C})/R_{\rm F} = 0.135$, while the width of the reverse shock region is only $x_{\rm R} = (R_{\rm C} - R_{\rm R})/R_{\rm F} = 0.011$. However, the density in the reverse shock is much larger, and we find that $M_{\rm R}/M_{\rm F} = 2.23$, where $M_{\rm R}$ and $M_{\rm F}$ are the masses enclosed in the reverse- and forward-shock regions, respectively. By construction, $M_{\rm F} = 4\pi K R_{\rm F}$. The resulting $(M_{\rm R} + M_{\rm F}) \approx 3.2 M_{\rm F}$ implies that the order of magnitude estimates identifying the total energy of the flash with $M_{\rm F}\dot{R}_{\rm F}^2/2$ (see e.g. Katz et al. 2010) should be corrected. While it is clear that the mass of the ejecta affected by the wind must be comparable to that of the swept-up wind, ignoring the mass enclosed in the reverse shock leads to a significant overestimate of the shock velocity.

The density profile in the self-similar solution can be integrated to find the normalized column density in the forward- and reverse-shock regions, which can then be used to estimate the optical depth and the diffusion time-scales. First, we define,

$$\hat{\tau}_{\rm F} = \frac{\int_{R_{\rm C}}^{R_{\rm F}} \rho(r){\rm d}r}{7 K R_{\rm F}^{-2}(R_{\rm F} - R_{\rm C})}; \quad \hat{\tau}_{\rm R} = \frac{\int_{R_{\rm R}}^{R_{\rm C}} \rho(r)\,{\rm d}r}{7 K R_{\rm F}^{-2}(R_{\rm C} - R_{\rm R})}. \tag{6}$$

The results for the self-similar solution depicted in Fig. 1 are $\hat{\tau}_{\rm F} \simeq 1.3$ and $\hat{\tau}_{\rm R} \simeq 4.2$. The total optical depth of the shock region is therefore

$$\tau_{\rm S} = \kappa(\hat{\tau}_{\rm F} x_{\rm F} R_{\rm F} + \hat{\tau}_{\rm R} x_{\rm R} R_{\rm F}) 7 K R_{\rm F}^{-2} \simeq 1.55 \kappa K R_{\rm F}^{-1}, \tag{7}$$

where we have assumed a uniform, frequency independent opacity, κ. The total diffusion time-scale in the shocked region, $t_{\rm DS}$ is then,

$$t_{\rm DS} = \tau_{\rm S} \frac{x R_{\rm F}}{c} \simeq 0.23 \frac{\kappa K}{c}. \tag{8}$$

Finally, the physical scales of the full solution are determined by the dimensional parameters, g and K. In particular, the velocity of the forward shock is related to its position by,

$$\dot{R}_{\rm F} = \frac{m-3}{m-2} \left(\frac{A_{\rm F} g^m}{K}\right)^{1/(m-3)} R_{\rm F}^{-1/(m-3)}, \tag{9}$$

where $A_{\rm F}$ is another constant that is extractable from the self-similar solution (Chevalier 1982); for $m = 10$ and $\gamma = 4/3$ we get $A_{\rm F} \approx 0.07$.

We note that the numerical values of x, $\chi_{\rm E}$, $\hat{\tau}_{\rm F}$ and $\hat{\tau}_{\rm R}$ are very weakly dependent on m. In the range of $m = 8$–12, we find that these values vary by no more than ± 20 per cent with respect to their values for $m = 10$, which we use for reference below. The value of $A_{\rm F}$ is not as well constrained, and changes within a factor of 2 in this range. However, as shown in Section 4, the final result is not sensitive to this uncertainty.

3 A SIMPLE PARAMETRIZATION OF THE BREAKOUT CONDITIONS

We now use the results of the previous section to estimate the shock-breakout features. We assume that prior to shock breakout the flow is approximately adiabatic in the shocked regions, and that leakage of radiation into the cold parts of the wind and ejecta is negligible. We discuss the validity of these assumptions below.

We take the total energy observed in the breakout flash, $E_{\rm X}$, to be comparable with the energy carried in radiation in the shocked region, $E_{\rm rad}$. Similarly the time-scale characterizing the postmaximum part of the light curve is determined by diffusion from the shock front through the unshocked wind, $t_{\rm diff}$. These associations are valid because the diffusion time of radiation in the shocked region is shorter than the time-scale for diffusion from the shock to the unshocked wind's photosphere. The optical depth from the shock front in the wind material is $\tau = \kappa K/R_{\rm F}$, and so the time-scale for diffusion from the shock front is

$$t_{\rm diff} \approx \tau \frac{R_{\rm F}}{c} = \frac{\kappa K}{c}, \tag{10}$$

or about four times longer than the time-scale for diffusion in the shocked region, given by equation (8). The opposite regime of $t_{\rm diff} \ll t_{\rm DS}$ would have been characterized by a longer, fainter light curve.

Observationally determined values of $E_{\rm X}$ and $t_{\rm diff}$ and the self-similar solutions provide the necessary relations for estimating the key properties of ejecta-wind configuration at breakout. First, using equation (10) the observed value of $t_{\rm diff}$ is sufficient to determine the value of the wind-density constant, K:

$$K = \frac{c t_{\rm diff}}{\kappa} = 1.5 \times 10^{14} \frac{t_{\rm diff,3}}{\kappa_{0.2}}\ {\rm g\ cm^{-1}}, \tag{11}$$

where $t_{\rm diff,3} = (t_{\rm diff}/10^3\ {\rm s})$ and $\kappa_{0.2} = (\kappa/0.2\ {\rm cm^2\ g^{-1}})$ (the fiducial opacity normalization is appropriate for wind material that is dominated by helium and heavier elements). The value of K for $t_{\rm diff,3} = 1$ corresponds to a wind mass-loss rate of about $3 \times 10^{-4}\ {\rm M_\odot\ yr^{-1}}$ for a wind velocity of 100 km s^{-1}.

The criterion for shock breakout is that the diffusion time be equal to dynamical time, $t_{\rm diff} = t_{\rm dyn} \equiv R_{\rm F}/\dot{R}_{\rm F}$. We use this relation to substitute the shock velocity from equation (4) for $t_{\rm diff}$, yielding

$$E_{\rm X} = \frac{72\pi c}{7\kappa} \chi_{\rm E} x R_{\rm S}^3 t_{\rm diff}^{-1}. \tag{12}$$

Using the predetermined values of $\chi_{\rm E}$ and x based on the self-similar solutions in Section 2, the breakout radius can be expressed in terms of $E_{\rm X}$ and $t_{\rm diff}$:

$$R_{\rm BO} = 5.4 \times 10^{12} \left(\frac{E_{X,47} t_{\rm diff,3}}{\kappa_{0.2}}\right)^{1/3} \left(\frac{x}{0.146}\right)^{-1/3} \left(\frac{\chi_{\rm E}}{0.9}\right)^{-1/3} {\rm cm}, \tag{13}$$

where $E_{\rm X,47} = (E_{\rm X}/10^{47}\ {\rm erg})$. We emphasize again that the specific values of x and $\chi_{\rm E}$ found in the self-similar solutions are weakly dependent on the exact value of the ejecta density profile, m. Combined with the fact that the breakout radius depends only on the

cubic roots of these numerical factors, we conclude that the the result of equation (13) is robust to uncertainties in the details of the ejecta profile.

Using the inferred values of the breakout radius and the wind-density coefficient, K, we can also express the masses of the wind material and the ejecta included in the forward and reverse shock, respectively. The mass in the forward shock is:

$$\frac{M_{\rm F}}{\rm M_\odot} = 5.1\times10^{-6}E_{X,47}^{1/3}t_{\rm diff,3}^{4/3}\kappa_{0.2}^{-4/3}\left(\frac{x}{0.146}\right)^{-1/3}\left(\frac{\chi_{\rm E}}{0.9}\right)^{-1/3}, \quad (14)$$

and $M_{\rm R}$ is about 2.23 times larger. It is a useful consistency check that the mass of the ejecta involved in the shock formation is significantly smaller than the total ejecta mass. An ejecta density profile of the form of equation (2) is only applicable to the edge of the progenitor envelope, where the initial density drops sharply with radius.

An important consequence of the estimate for the breakout radius is the corresponding shock velocity. The value of this velocity (normalized by c) is, $\beta_{\rm s}\sim 0.18E_{\rm rad,47}^{1/3}t_{\rm diff,3}^{-2/3}$. This relates the observed global features of the light curve and the spectrum, since for $\beta > 0.07$ the photon generation rate in the shocked region is insufficient to establish a Planck distribution within the shock width (Katz et al. 2010). The emergent spectrum in that regime is dominated by harder ($\geq$1 keV) X-ray photons than a blackbody, since the same amount of energy is shared by fewer photons. If, on the other hand, $\beta_{\rm s} < 0.07$, the flash should exhibit a blackbody spectrum with a temperature of

$$T_{\rm BB}\approx 2.64\times10^{5}E_{\rm rad,47}^{1/12}t_{\rm diff,3}^{-5/12}\kappa_{0.2}^{1/6}\left(\frac{x}{0.146}\right)^{1/6}\left(\frac{\chi_{\rm E}}{0.9}\right)^{1/6}{\rm K}, \quad (15)$$

assuming that the characteristic luminosity is $L=4\pi R_{\rm BO}^2\sigma T_{\rm BB}^4\sim E_{\rm X}/t_{\rm diff}$.

Some cautionary remarks should be mentioned about our results. First, a useful aspect of equation (13) is that for the reference values of $E_{\rm rad}\sim10^{47}$ erg and $t_{\rm diff}\sim10^3$ s, the light crossing time at the breakout radius is about 18 per cent of the diffusion time. Therefore, the geometric time delay due to the light crossing time will have a secondary, but not negligible, effect on the earlier part of the flash light curve. Another caveat is related to our assumption that the kinetic energy of the shocked region (and that of the unshocked ejecta) will not be converted into internal energy over the time-scale of the breakout flash. We expect this approximation to be valid, since the shocked region would slow down significantly only after it sweeps up an additional wind mass comparable to its own, $(M_{\rm R}+M_{\rm F})=3.2\times4\pi K R_{\rm BO}$ (see Section 2). Hence, it takes at least several dynamical times, or diffusion times, to convert kinetic energy to internal energy. Moreover, the kinetic energy of the shocked material, $E_{\rm kin}\approx\frac{1}{2}(M_{\rm R}+M_{\rm F})(\dot{R}_{\rm F}/7)^2$, is only about 10 per cent of its internal energy, and so the addition to the available energy would generate at most a 3 per cent correction in the value of $R_{\rm BO}$ in equation (13). The main reservoir of kinetic energy lies in the yet unshocked ejecta, but this region takes even longer to slow down and is initially hidden behind larger optical depths.

Another secondary effect we have neglected is the possible acceleration of gas ahead of the shock by radiation which escapes the shocked region. While an exact calculation of the extent of this effect requires a radiation-hydrodynamics simulation, it is straightforward to demonstrate that relative to velocities $\gtrsim10^9\,{\rm cm\,s^{-1}}$ significant acceleration of wind material at any given radius below $R_{\rm BO}$ cannot take place before the shock overtakes that radius. It is also noteworthy that the optical depth of the unshocked ejecta is quite large, so radiative effects should not increase the width of the reverse shock significantly prior to breakout.

A more serious concern is to what extent the ejecta is in a cold, power-law density state prior to breakout. For compact progenitors with a radius $R_\star\sim10^{11}$ cm, the reference values give $R_{\rm BO}/R_\star\approx54$. While this ratio is sufficiently large to justify neglecting the progenitor radius as a relevant scale in the solution, it is not obvious that the density profile should already settle at $R_{\rm BO}$ into the asymptotic form we assumed in equation (2). Originally, the supernova shock wave deposits in the outer envelope ~six times as much internal energy as kinetic energy. For spherical adiabatic expansion, the internal energy declines as $E\sim r^{-1}$, so for $(E_{\rm rad,47}t_{\rm diff,3})<1$ the ejecta can still be 'lukewarm' rather than cold, implying that the ejecta density profile may still be developing, and perhaps that the reverse shock may not be very strong. This might lead to some deviation of the gas dynamics from our simple model.

4 A SIMPLE PARAMETRIZATION OF THE EXPLOSION PROPERTIES

We next incorporate the properties of the explosion into our model. This can be done by relating the two quantities describing the ejecta profile, g and m, to the explosion parameters. In practice, obtaining such a relation requires a specific model for the fast material leading the ejecta, and we use the standard model of Matzner & McKee (1999). In this model, the original density in pre-explosion outer layers of the star, ρ_0, is a simple function of the relative distance from the edge of the star,

$$\rho_0(r_0)=\rho_\star\delta^n;\quad \delta=1-r_0/R_\star, \quad (16)$$

where $R_\star$ is the outer radius of the progenitor and and r_0 is the radial position within the progenitor. The power n is a constant which depends on the assumed physics of the envelope – $n=3$ for a convective envelope and $n=3/2$ for a radiative one, and the density scale, $\rho_\star$, depends on the details of the progenitor structure.

Given this initial density profile, Matzner & McKee (1999) have shown that after the passage of the shock the velocity of the material in the very outer envelope follows an approximate dependence on the energy of the explosion, E, and the total mass of the ejecta, M:

$$v(r_0)=A_{\rm v}\left(\frac{E}{M}\right)^{1/2}\left(\frac{4\pi}{3f_\rho}\right)^{\beta}\delta^{-\beta n}, \quad (17)$$

where $\beta\approx0.19$ is practically independent of the details of the progenitor and the explosion, and $f_\rho\equiv\rho_\star/\bar{\rho}$, where $\bar{\rho}=3M/4\pi R_\star^3$ is the average mass density within the star. The asymptotic value of the coefficient $A_{\rm v}$ is $\sim2A_{\rm v,S}$, where $A_{\rm v,S}\approx0.79$ is the appropriate value for the *shock* velocity profile at the onset of the explosion. If the wind were dynamically unimportant and the ejecta could reach reach this asymptotic velocity profile, then the resulting density profile obtains the form (Rabinak & Waxman 2011),

$$\rho(\delta_{\rm m},r)=-\frac{M}{4\pi r^3}\frac{(n+1)}{\beta n}\delta_{\rm m}, \quad (18)$$

where $\delta_{\rm m}(\delta)$ is the Lagrangian mass fraction of an element of the ejecta which was initially at δ in the pre-explosion profile. With $\delta_{\rm m}=3f_\rho\delta^{(n+1)}/(n+1)$ and approximating that an element with $\delta_{\rm m}$ reaches a radius r at a time of $t\simeq r/v$ we arrive at an expression of the ejecta in the form of equation (2):

$$\rho(r,t)=\left(\frac{4\pi}{3f_\rho}\right)^{1/n}(A_{\rm v})^{2\theta}E^{\theta}M^{1-\theta}r^{-m}t^{m-3}, \quad (19)$$

where $\theta = (n+1)/(2\beta n)$, and

$$m = -3 - \frac{n+1}{\beta n}. \quad (20)$$

Again, we assume that the ejecta is cold and has developed the density profile of equation (2). Joining equations (9) and (19) sets a quantitative constraint on the combination of the explosion energy, E, and the ejecta mass, M. Specifically for $\beta = 0.19$ and $n = 3$ we have $m \simeq 10$ and $\theta \simeq 3.5$, and with the aid of the characteristic values derived in the self-similar solution we arrive (after some algebra) at the final result:

$$\left(\frac{E}{10^{51}\,\mathrm{erg}}\right)\left(\frac{M}{\mathrm{M}_\odot}\right)^{-5/7} \simeq 0.8 A_{\rm v}^{-2} f_\rho^{2/21}\left(\frac{A_{\rm F}}{0.07}\right)^{-2/7} \kappa_{0.2}^{10/21} E_{\rm rad,47}^{16/21} t_{\rm diff,3}^{-20/21}. \quad (21)$$

Although this equation is approximate, it implies that within the framework of our model, the plausible range of values for the entire prefactor in equation (21) is rather limited. The values of x and $\chi_{\rm E}$ are tightly constrained in the self-similar solution, and do not introduce a significant uncertainty. The coefficient $A_{\rm F}$ which does depend on the power of the ejecta density profile is suppressed by the 2/7 power, and the unknown factor f_ρ is suppressed by the 2/21 power. Finally, $A_{\rm v} \approx 1.6$ for ejecta that has approached its asymptotic velocity. The resulting equation can be applied as a sanity check for the value of the product $EM^{-5/7}$, when a flash is suspected to be the result of a supernova-wind breakout scenario.

5 THE X-RAY FLASH IN XRO080109/SN2008D

We now examine the predictions of our model for the best candidate to date of an X-ray flash due to shock breakout in a wind XRO080109, associated with the Type Ibc supernova SN2008D (Soderberg et al. 2008). Whereas a similar analysis can be applied to the case of GRB060218/SN2006aj, this source requires relativistic expansion (Li 2007), and possibly a significant deviation from spherical symmetry (Waxman et al. 2007), so we do not consider it here.

The bright X-ray transient XRO080109 was serendipitously discovered during a scheduled *Swift* Telescope observation of the galaxy NGC2770 (at a distance of ∼27 Mpc). The observed spectrum shows a non-thermal shape with a power-law frequency dependence of the photon number flux per unit frequency, $N_\nu \propto \nu^{-\Gamma}$ with $\Gamma = 2.3 \pm 0.3$, through the observed range of X-ray energies, 0.3–10 keV. The follow-up observation by the Ultraviolet/Optical Telescope (UVOT) on-board *Swift* discovered a counterpart Type Ib supernova, denoted SN2008D. Analyses of the main light curve of SN2008D (Mazzali et al. 2008; Modjaz et al. 2009; Tanaka et al. 2009) favour an underlying explosion of a compact progenitor, presumably a Wolf–Rayet star due to the lack of hydrogen lines in the light curve. A consistent result was found by Rabinak & Waxman (2011) in their analysis of the early UV/optical light curve, in which they inferred a initial progenitor radius of $\sim 10^{11}$ cm. Note that for such a compact progenitor, a typical wind velocity should be of the order of 1000 km s^{-1} (similar to the escape velocity). The light curve of XRO080109 displayed a rapid rise and an exponential decline, with an e-folding time in the declining phase of approximately $t_{\rm e} = 130$ s. Such a time-scale is too long to be consistent with breakout through the surface of a bare star, and the most plausible explanation links this decline with the diffusion of the radiation from the shock through the unshocked wind, $t_{\rm e} = t_{\rm diff}$, which we will use below. For an alternative interpretation, that the light curve was shaped by an aspherical explosion, see Couch et al. (2010).

Quantitative estimates of the total energy of the burst (assuming isotropic emission) depend on the modelling of the column density near the source and extinction; Soderberg et al. (2008) estimated the total energy in the burst to be $E_{\rm X} \approx 2 \times 10^{46}$ erg, for which the appropriate breakout radius arising from equation (13) is $R_{\rm BO} \approx 1.6 \times 10^{12}$ cm. For the lower value of $E_{\rm X} \approx 6 \times 10^{45}$ erg inferred by Modjaz et al. (2009), the breakout radius is reduced to $R_{\rm BO} \approx 1.1 \times 10^{12}$ cm. In either case, the breakout must have occurred in a wind rather than on the surface of a bare Wolf–Rayet progenitor. Our result is consistent with the lower limit of 7×10^{11} cm for the breakout radius found by Soderberg et al. (2008), based on the fact that the thermal component of the X-ray flash lies below the XRT low-energy cut-off of ∼0.1 keV.

We note that the diffusion time-scale indicates a density profile with $K \simeq 1.95 \times 10^{13}$ g cm^{-1}, corresponding to $\dot{M}/v_{\rm w} \approx 3.85 \times 10^{-4}\,\mathrm{M}_\odot\,\mathrm{yr}^{-1}/(1000\,\mathrm{km\,s}^{-1})$. This value is an order of magnitude larger than the range estimated by Soderberg et al. (2008) and Chevalier & Fransson (2008) from the radio observations of SN2008D, assuming a 10 per cent efficiency in magnetic field production behind the shock front. Taken at face value, our result implies a lower efficiency for magnetic field production, or an enhanced mass-loss rate just prior to explosion, or both. We note that that Soderberg et al. (2008) estimated a low $\dot{M}$ also from the breakout flash, but this discrepancy is alleviated once our value for the breakout radius is used (rather than their lower limit), along with with a specific opacity of $\kappa = 0.2\,\mathrm{cm^2\,g^{-1}}$ and a remaining optical depth of $\tau = 2$–3 in the unshocked wind.

The corresponding total amount of mass involved in the forward and reverse shocks at breakout comes out to be of the order of $10^{-7}\,\mathrm{M}_\odot$. Although small, this mass is several orders of magnitude larger than that enclosed in the last few optical depths of a bare Wolf–Rayet star with $R_\star \approx 10^{11}$ cm (Matzner & McKee 1999), again supporting the wind breakout scenario.

Finally, the combination of explosion energy and ejected mass in equation (21) yields $(E/10^{51}\mathrm{erg})(M/\mathrm{M}_\odot)^{-5/7} \approx 0.26$–$0.64\,f_\rho^{2/21}$ for the total energies of $E_{\rm X} = 0.6$–2×10^{46} erg. Depending on the value of f_ρ, this result appears to lie between the combination originally suggested by Soderberg et al. (2008) of $(E/10^{51}\,\mathrm{erg}) = 2$, $(M/\mathrm{M}_\odot) = 5$, and the more energetic explosions inferred later by Mazzali et al. (2008) and Tanaka et al. (2009), $(E/10^{51}\,\mathrm{erg}) = 6$, $(M/\mathrm{M}_\odot) = 6$–8.

We caution that $(R_{\rm BO}/R_\star) \sim 11$–$16(R_\star/10^{11}\,\mathrm{cm})^{-1}$ is modest, and so the deviation from the cold ejecta model may be significant (and even more so if the progenitor radius was a few 10^{11} cm). This deviation does not change much the energetics of the model, which is why the general results are consistent with shock breakout in a wind, but the details of the shock structure are most likely different than those predicted by our solution. A further complication will arise from the wind density profile, which close to the star may be significantly steeper than a $\rho \sim r^{-2}$ dependence (Li 2007). If the shocked wind material is dominated by this component, additional quantitative corrections must be included in our model. Such a wind structure may also provide a natural explanation the relatively large mass-loss rate we required assuming $\rho \sim r^{-2}$ throughout the entire wind.

Another point of interest is that the shock velocity at breakout we find for SN2008D is quite large, with $\beta \approx 0.3$–0.4. This range is still consistent with our non-relativistic approach, and is also in agreement with the velocity range inferred from later very long baseline interferometry (VLBI) measurements (Bietenholz,

Soderberg & Bartel 2009). However, given the relatively small breakout radius, it is most likely an upper limit: at $(R_{\rm BO}/R_\star) \approx$ 10–15 the ejecta may still be carrying a significant fraction of its initial internal energy that was not converted to kinetic energy. We also emphasize that if the optical depth at breakout is only $\tau = \beta^{-1} \approx$ 2.5–3, the diffusion approximation becomes questionable. Finally, at $\beta > 0.2$ pair creation in the shock is non-negligible (Weaver 1976; Budnik et al. 2010; Katz et al. 2010), causing the equation of state to deviate from a pure $\gamma = 4/3$ ideal gas. None the less, our simple model is robust enough to demonstrate that the shock velocity in SN2008D was large enough for the photon energy distribution not to be Planckian, leading naturally to the observed non-thermal X-ray spectrum.

6 CONCLUSIONS AND DISCUSSION

We have presented a simple model for the properties of shock breakout in a supernova explosion embedded within an optically thick wind. By assuming that the ejecta and wind form a forward–reverse shock structure (Chevalier 1982), we have shown that the breakout radius can be estimated based on the observationally determinable values of the total energy in the flash and the diffusion time-scale from the shock to the wind's photosphere. Among other things, we demonstrated that the time-scale for photon diffusion in the shocked region is shorter than the time-scale for photon diffusion from the shock to the photosphere, justifying the underlying assumption that breakout will manifest itself as a brief flash even in the presence of an optically thick wind. We also found that if the ejecta time-dependent density profile is derived from the initial progenitor model of Matzner & McKee (1999), the combination of explosion energy and ejecta mass can be estimated from the observed quantities of the shock breakout. For a low flash energy and long diffusion time, a blackbody spectrum is expected to emerge. In the opposite regime, free–free emission cannot generate a sufficient number photons to establish a thermal spectrum during the shock passage (Katz et al. 2010).

While limited by its simplifying assumptions, our model describes the general features of a shock breakout in a wind around an exploding Wolf–Rayet star, characterizing a Type Ibc supernova. We applied our model to the X-ray flash observed in association with SN2008D (Soderberg et al. 2008) and found sensible values for the shock-breakout radius ($\sim$1.1–1.6 $\times$ 10^{12} cm) as well as the properties of the entire explosion. However, such a breakout radius is probably not sufficiently larger than the progenitor radius for our model to be fully applicable. It is therefore possible that we are overestimating the shock velocity at breakout, which we found to be $\beta_{\rm s} \sim$ 0.3–0.4. None the less, our model clearly demonstrates that if XRO080109 was indeed shock breakout in SN2008D, the shock velocity was certainly large enough to prevent a blackbody spectrum from developing, in agreement with observations.

Additional note: after the completion of this paper a related preprint was posted by Chevalier & Irwin (2011). They too use the self-similar solution to assess the total energy available for shock breakout through a wind, but their work focuses on a different setting involving a red supergiant exploding into a much denser wind. In their case the typical breakout radius is $R_{\rm BO} \sim 10^{15}$ cm and the mass of the ejecta involved in the shock comes out to be $>1\,{\rm M}_\odot$; hence the assumption of a simple power-law dependence for the density of the ejecta (equation 2) may not be adequate (see Section 3).

ACKNOWLEDGMENTS

We wish to thank Alicia Soderberg for valuable comments and Udi Nakar and Eli Waxman for helpful discussions. We also thank Roger Chevalier for his helpful comments as the referee of this paper. SB thanks the Institute for Theory & Computation (ITC) at Harvard University for its kind hospitality. This work was supported in part by NSF grant AST-0907890 and NASA grants NNX08AL43G and NNA09DB30A.

REFERENCES

Bietenholz M. F., Soderberg A. M., Bartel N., 2009, ApJ, 694, L6
Budnik R., Katz B., Sagiv A., Waxman E., 2010, ApJ, 725, 63
Campana S. et al., 2006, Nat, 442, 1008
Chevalier R. A., 1982, ApJ, 258, 790
Chevalier R. A., 1983, ApJ, 272, 765
Chevalier R. A., 1992, ApJ, 394, 599
Chevalier R. A., Fransson C., 2008, ApJ, 683, 185
Chevalier R. A., Irwin C. M., 2011, ApJ, 729, L6
Colgate S. A., 1974, ApJ, 177, 333
Couch S. M., Pooley D., Wheeler J. C., Milosavljević M., 2011, ApJ, 727, 104
Falk S. W., 1978, ApJ, 225, L133
Gezari S. et al., 2008, ApJ, 683, L131
Gezari S. et al., 2010, ApJ, 720, L77
Katz B., Budnik R., Waxman E., 2010, ApJ, 716, 781
Klein R. I., Chevalier R. A., 1978, ApJ, 223, L109
Li S. W., 2007, MNRAS, 375, 240
Matzner C. D., McKee C. F., 1999, ApJ, 510, 379
Mazzali P. A. et al., 2008, Sci, 321, 1185
Modjaz M. et al., 2009, ApJ, 702, 226
Nakar E., Sari R., 2010, ApJ, 725, 904
Ofek E. O. et al., 2010, ApJ, 724, 1396
Parker E. N., 1963, Interplanetary Dynamical Processes. Interscience, New York
Rabinak I., Waxman E., 2011, ApJ, 728, 63
Soderberg A. M. et al., 2008, Nat, 453, 469
Tanaka M. et al., 2009, ApJ, 692, 1131
Weaver T. A., 1976, ApJS, 32, 233
Waxman E., Mészáros P., Campana S., 2007, ApJ, 32, 233

This paper has been typeset from a TEX/LATEX file prepared by the author.